Acta Biomaterialia xxx (2014) xxx–xxx

Contents lists available at ScienceDirect

Acta Biomaterialia

journal homepage: www.elsevier.com/locate/actabiomat

Parathyroid hormone-related protein (107-111) improves the bone regeneration potential of gelatin–glutaraldehyde biopolymer-coated hydroxyapatite

Daniel Lozano [a,b], Sandra Sánchez-Salcedo [c,e], Sergio Portal-Núñez [a], Mercedes Vila [c,e], Ana López-Herradón [a], Juan Antonio Ardura [a], Francisca Mulero [d], Enrique Gómez-Barrena [b], María Vallet-Regí [c,e,*,1], Pedro Esbrit [a,1]

[a] Laboratorio de Metabolismo Mineral y Óseo, Instituto de Investigación Sanitaria (IIS)-Fundación Jiménez Díaz and Instituto de Salud Carlos III-RETICEF, Avenida Reyes Católicos, 2, 28040, Madrid, Spain
[b] Grupo de Investigación de Cirugía Osteo-Articular, Instituto de Investigación Hospital Universitario La Paz (IdiPAZ), Paseo de la Castellana 261, 28046, Madrid, Spain
[c] Departamento de Química Inorgánica y Bioinorgánica, Facultad de Farmacia, Universidad Complutense de Madrid (UCM), Instituto de Investigación Sanitaria Hospital 12 de Octubre i+12, Pza. Ramón y Cajal s/n, 28040 Madrid, Spain
[d] Unidad de Imagen Molecular, Centro Nacional de Investigaciones Oncológicas (CNIO), Calle de Melchor Fernandez Almagro3, 28029, Madrid, Spain
[e] Centro de Investigación perteneciente a la Red de Bioingeniería, Biomateriales y Nanomedicina, Zaragoza, Spain

ARTICLE INFO

Article history:
Received 20 December 2013
Received in revised form 21 March 2014
Accepted 24 March 2014
Available online xxxx

Keywords:
Macroporous scaffolds
Hydroxyapatite
PTHrP (107-111)
In vivo bone regeneration
Rat

ABSTRACT

Biopolymer-coated nanocrystalline hydroxyapatite (HA) made as macroporous foams which are degradable and flexible are promising candidates as orthopaedic implants. The C-terminal (107-111) epitope of parathyroid hormone-related protein (PTHrP) exhibits osteogenic properties. The main aim of this study was to evaluate whether PTHrP (107-111) loading into gelatin–glutaraldehyde biopolymer-coated HA (HA_{Glu}) scaffolds would produce an optimal biomaterial for tissue engineering applications. HA_{Glu} scaffolds with and without PTHrP (107-111) were implanted into a cavitary defect performed in both distal tibial metaphysis of adult rats. Animals were sacrificed after 4 weeks for histological, microcomputerized tomography and gene expression analysis of the callus. At this time, bone healing occurred only in the presence of PTHrP (107-111)-containing HA_{Glu} implant, related to an increase in bone volume/tissue volume and trabecular thickness, cortical thickness and gene expression of osteocalcin and vascular cell adhesion molecule 1, but a decreased gene expression of Wnt inhibitors, SOST and dickkopf homolog 1. The autonomous osteogenic effect of the PTHrP (107-111)-loaded HA_{Glu} scaffolds was confirmed in mouse and human osteoblastic cell cultures. Our findings demonstrate the advantage of loading PTHrP (107-111) into degradable HA_{Glu} scaffolds for achieving an optimal biomaterial that is promising for low load bearing clinical applications.

1. Introduction

The number of traumatic and non-traumatic fractures, particularly if producing secondary bone defects, has increased enormously in the past few decades, associated with the increase in lifespan in our societies [1]. In this context, the development of optimal strategies to accelerate bone repair after fracture is likely to have a great socioeconomic impact.

Bone healing involves a variety of cellular and molecular events that lead to new bone formation [2,3]. This process recapitulates most of the features of normal bone development during embryogenesis, but it is highly influenced by factors such as mechanical loading and the relative abundance of osteoprogenitors (e.g. low in older patients). In addition, injured bone tissue revascularization, providing oxygen, nutrients and cell precursors, is critical for bone healing [4]. However, the resolution of fractures often requires the use of synthetic materials as implants to replace bone tissue damage.

Different types of ceramics have been widely used in this respect, because of their similarity with the mineral component of natural bone [5,6]. Current interest is focused on bioactive and biodegradable bioceramics as scaffolds exhibiting suitable osteointegration and osteoconductive features in bone tissue engineering applica-

* Corresponding author at: Dto. Química Inorgánica y Bioinorgánica, Facultad de Farmacia – U.C.M., Pza. Ramón y Cajal s/n, 28040 Madrid, Spain. Tel.: +34 913941843; fax: +34 913941786.
E-mail address: vallet@ucm.es (M. Vallet-Regí).
[1] These authors have the same senior status in this work.

http://dx.doi.org/10.1016/j.actbio.2014.03.025
1742-7061/

tions [7,8]. In this line, hydroxyapatite (HA) and other calcium phosphates are widely used as degradable scaffolds with interconnected porosity, including macropores in the 1–500 μm range allowing cellular internalization [3]. Recently, three-dimensional HA foams with a high degree of porosity were prepared by sol–gel routes, and coated with gelatin–glutaraldehyde biopolymers to give them flexibility and easy manipulation in orthopaedic applications [9–11]. These materials were shown to allow cellular colonization and excellent biocompatibility both in vitro and in vivo [11,12].

The increasing importance of growth factors to improve the osteoinductive properties of implanted scaffolds is well recognized [13]. In fact, these agents (now represented mainly by bone morphogenetic proteins) comprise about 20% of the whole orthopaedic market in the US – a 3-fold higher figure than the current percentage of resorbable implants – and this percentage is expected to grow rapidly [14]. An emerging factor in this regard is parathyroid hormone-related protein (PTHrP), the N-terminal fragment of which has been shown to induce bone anabolic actions in rodents and humans upon systemic daily administration [15,16]. In addition, the C-terminal 107-111 domain (also known as osteostatin) of PTHrP also exhibits osteogenic features in vitro, and stimulates bone accrual in vivo [17–25]. Of note, we recently showed that loading non-degradable Si-based ceramics with the latter pentapeptide gives them osteogenic and angiogenic features both in vitro and in vivo as implants in a cavitary defect in the rabbit femur [26–29]. These effects of osteostatin were thought to be due to its release into the local environment, because this type of ceramic elicits the formation of a fibrous capsule that hampers close contact between the implant and the surrounding tissue [27,29]. In any event, these recent observations point to PTHrP (107-111) as an interesting peptide in a bone tissue engineering scenario.

In the present study, using a rat bone defect model, we evaluated two combined approaches, i.e. the use of degradable HA_{Glu} foams and the putative advantage of loading PTHrP (107-111) into these scaffolds, to produce an optimal biomaterial for low load bearing clinical applications.

2. Materials and methods

2.1. Preparation of carbonated hydroxyapatite/gelatin scaffolds

Three-dimensional HA foams were synthesized and shaped in a one-step process following a sol–gel technique [9], using Pluronic F127 (EO106PO70EO106) as a macropore inducer, followed by an accelerated evaporation-induced self-assembly method [10]. Briefly, HA was synthesized from the reaction of calcium nitrate tetrahydrate and triethylphosphite (TIP; Aldrich, Steinheim, Germany), using a molar ratio of F127:TIP of 11. The resulting foams were coated by immersion in a 1.2% (w/v) type A gelatin cross-linked with 0.05% w/v glutaraldehyde solution and then lyophilized for 24 h, as reported elsewhere [30]. Scanning electron microscopy (SEM) in a JEOL 6400 microscope (Tokyo, Japan) was used to characterize the macroporous 3-D architecture of the gelatin–glutaraldehyde biopolymer-coated HA (HA_{Glu}) foams and X-ray diffraction (XRD) in a Philips X'Pert diffractometer using Cu K_α radiation. Supplementary details of the characterization of these foams have been reported previously [9–11]. HA_{Glu} scaffolds for in vivo and in vitro assays were prepared as samples of 7 mg (3 mm in height, 3 mm in depth and 3 mm in width) with a ratio of 58 mg mm^{-3}.

HA_{Glu} scaffolds were loaded with synthetic PTHrP (107-111) (Bachem, Bubendorf, Switzerland) by soaking them in a solution of the peptide (at 100 nM) in 1 ml of phosphate-buffered saline (PBS) solution (pH 7.4) with constant shaking at 4 °C for 24 h. Peptide release from the loaded material was assessed by including a radiotracer together with the cold peptide during PTHrP (107-111) loading, as described elsewhere [26]. The radioactivity released into the incubation medium was sequentially monitored by counting in a γ-spectrometer. By using this method, the mean uptake of PTHrP (107-111) by these scaffolds after 24 h of loading was 60%, equivalent to 0.7 ng of peptide per mg of scaffold. Meanwhile, 80% of this amount was released to the surrounding medium within 1 h, and virtually 100% at 48 h. It was previously shown that minor amounts of this peptide (in the sub-nanomolar range) still sustained biological activity [18,23,25,26].

2.2. In vivo rat model of bone healing

Our protocol, using a limited number of male Wistar rats (6 months of age; $n = 5$ per experimental group) was approved by the Institutional Animal Care and Use Committee at the IIS-Fundación Jiménez Díaz, according to the European Union guidelines for decreasing the pain and suffering of the animals. The rats were placed in cages under standard conditions (room temperature 20 ± 0.5 °C, relative humidity 55 ± 5% and illumination with a 12 h/12 h light/dark photoperiod), given food and water ad libitum and allowed to move without restriction. Surgical interventions were performed under aseptic conditions and general anaesthesia was induced by injection of xylacine (10 mg kg^{-1}) and ketamine (25 mg kg^{-1}). Both knees were shaved, and a transcortical defect was generated by drilling a hole (2 mm in diameter and 3 mm in depth) through the cortex of both distal tibial metaphyses, using continuous irrigation with physiological saline to prevent bone necrosis. The healing response in this simple defect recapitulates that of a stabilized fracture, minimizing animal morbidity, trauma and infection [31,32]. The unloaded HA_{Glu} scaffolds were implanted into the left tibial defect, whereas the right tibial defect received the PTHrP-derived pentapeptide-loaded scaffold. Rats were sacrificed after 4 weeks for histological, microcomputerized tomography (μCT) and gene expression analysis of the callus.

2.3. μCT analysis

Both tibiae were scanned using GE eXplore Locus μCT scanner (GE Healthcare, London, Canada). The X-ray tube settings were 80 kV of energy and 450 μA of current. The μCT image acquisition consisted of 400 projections collected in one full rotation of the gantry. The resulting raw data were reconstructed using a filtered back-projection algorithm to a final image with a resolution of 93 μm in all three spatial dimensions. The reconstructed images were viewed and analysed using MicroView software, version 2.2 with Advanced Bone Analysis plus (GE Healthcare). Bone volume/tissue volume (BV/TV) as well as trabecular and cortical thickness (Tb.Th and Ct.Th, respectively) were calculated.

2.4. Histological evaluation

Tibiae were removed and fixed in 10% neutral formaldehyde, followed by decalcification with Osteosoft (Merck, Madrid Spain) for 4 weeks. Bone specimens were dehydrated before paraffin embedding using a Leica TP 1020 tissue processor. All histological and immunohistochemical determinations were carried out onto sagittal 4 μm sections of each bone sample in a Zeiss Axiophot optical microscope (Carl Zeiss, Oberkochen, Germany). For histological analysis, haematoxylin & eosin and Masson's trichromic staining were used. Osteoblasts (cubic cells adjacent to the bone surface) and osteoclasts (polynucleated cells with a rough border close to bone surfaces) were also quantified in the same trabecular area (5 mm^2) around the scaffold, loaded or not with PTHrP (107-111), in which μCT evaluation was carried out as described above.

Please cite this article in press as: Lozano D et al. Parathyroid hormone-related protein (107-111) improves the bone regeneration potential of gelatin–glutaraldehyde biopolymer-coated hydroxyapatite. Acta Biomater (2014), http://dx.doi.org/10.1016/j.actbio.2014.03.025

Evaluations were performed by at least two independent observers in a blinded fashion for each rat.

2.5. Cell culture studies

Cell culture experiments were performed using the well-characterized mouse osteoblastic cell line MC3T3-E1 (subclone 4, CRL-2593; ATCC, Mannassas, VA), which responds to C-terminal PTHrP peptides [25,26,33,34]. The tested scaffolds were placed into each well of 6- or 24-well plates before cell seeding. MC3T3-E1 cells were then plated at a density of 10,000 cells cm^{-2} in 2 ml of osteogenic medium consisting of α-minimum essential medium containing 10% heat-inactivated foetal bovine serum (FBS), 50 μg ml^{-1} ascorbic acid, 10 mM β-glycerol-2-phosphate and 1% penicillin–streptomycin at 37 °C in a humidified atmosphere of 5% CO_2, and incubated for different times. Human osteoblast-like (hOB) cells, isolated from trabecular bone explants obtained from knee samples discarded at the time of surgery on two osteoarthritic subjects (aged 69 and 80 years) [34], were cultured in Dulbecco's modified Eagle's medium containing 15% FBS and the same aforementioned supplements for 12 days. Some wells contained no scaffolds as controls. Medium was replaced every other day.

Cell proliferation was assessed after MC3T3-E1 cell incubation with the different materials for 4 days. At this time, 10 vol.% Alamar blue solution (AbD Serotec, Oxford, UK) was added to the cell culture. Four hours later, 1 ml samples of the cell-conditioned medium were added to a 24-well plate and the fluorescence intensity was measured using excitation and emission wavelengths of 540 and 620 nm, respectively. Following incubation with the tested materials for 4 days, the cells were washed with PBS and the alkaline phosphatase (ALP) activity was measured in cell extracts obtained with 0.1% Triton X-100 using p-nitrophenylphosphate as the substrate, as described previously [26,34]. The ALP activity was normalized to cell protein content, determined by the bicinchoninic acid (Thermo Scientific, Rockford, IL, USA) method with bovine serum albumin as standard. Matrix mineralization in MC3T3-E1 or hOB cells exposed to the tested materials for 12 days was determined using Alizarin S red staining, with the absorbance at 620 nm being measuring as described previously [26,34].

2.6. Real-time PCR

Total RNA was isolated from osteoblastic MC3T3-E1 cells and the rat tibia callus by a standard procedure (Trizol, Invitrogen, Groningen, The Netherlands), and gene expression was analysed by real-time PCR using an ABI PRISM 7500 system (Applied Biosystems, Foster City, CA), as reported [26,34]. Real-time PCR was done using *Sybr premix ex Taq* (Takara, Otsu, Japan) and the following rat-specific primers: 5′-GCTGCATGAGGCACGCTAT-3′ and 5′-AGGGCATGCATATTCCGTTT-3′ (dickkopf homolog 1, DKK-1); or 5′-GAGTACCCAGAGCCTCCTCA-3′ and 5′-AGCACACCAACTCGGTGA-3′ (Sost). Osteocalcin (OC), osteoprotegerin (OPG), receptor activator of nuclear factor-κB ligand (RANKL), vascular endothelial growth factor (VEGF) and vascular cell adhesion molecule 1 were analysed using unlabelled mouse- or rat-specific primers and TaqMan^{MGB} probes obtained by Assay-by-Design^{SM} (Applied Biosystems). The mRNA copy numbers were calculated for each sample by using the cycle threshold (*Ct*) value. 18S rRNA (a housekeeping gene) was amplified in parallel with tested genes. The number of amplification steps required to reach an arbitrary intensity *Ct* was computed. The relative gene expression was represented by $2^{-\Delta\Delta Ct}$, where $\Delta\Delta Ct = \Delta Ct_{\text{target gene}} - \Delta Ct_{18S}$. The fold change for the treatment was defined as the relative expression compared with control, calculated as $2^{-\Delta\Delta Ct}$, where $\Delta\Delta Ct = \Delta Ct_{\text{reatment}} - \Delta C_{\text{control.}}$

2.7. Statistical analysis

Results are expressed as mean ± standard error of the mean (SE). Statistical evaluation was carried out with non-parametric Kruskal–Wallis test and the post hoc Dunn's test or Mann–Whitney *U*-test, when appropriate. A value of $p < 0.05$ was considered significant.

3. Results

3.1. Characterization of HA_{Glu} scaffolds

The preparation technique employed on HA_{Glu} foams enables one not only to synthesize and fabricated macroporous scaffolds in a one-step process, but also to create a hierarchical interconnected structure from the macroporous to the mesoporous range. HA_{Glu} foams take up Trypan blue stain by diffusion through the pores, indicating good interconnected porosity (Fig. 1A). SEM micrographs of HA_{Glu} foams show interconnected macroporosity with a porosity range of 1–400 μm (Fig. 1B). The XRD pattern corresponds to pure nanocrystalline HA (ICDD PDF 9-432) (Fig. 1C). The average crystallite size calculated was 20 nm, based on all the reflections by Rietveld refinement [35]. As previously reported, transmission electron microscopy indicated a mesoporous network with a pore size of 10–15 nm (Supplementary Fig. S1). The total porosity measured by Hg intrusion of three representative HA_{Glu} specimens is approx. 70% (Supplementary Fig. S2). Thermogravimetric analyses of these samples confirmed their content of 80% wt. HA and 20% wt. gelatin (Supplementary Fig. S3). These scaffolds behave as a hydrogel, i.e. the network is able to absorb fluid maintaining its overall structure. The swelling ratio (*W*) was calculated as (%): $100 \times (Wt - Wd)/Wd$, where *Wd* is the weight of dried foam and *Wt* is the weight of hydrated foam. HA_{Glu} foams have a *W* of 400% wt. when immersed in aqueous solution due to the hydrophilic nature of glutaraldehyde-crosslinked gelatin (Supplementary Fig. S4).

3.2. PTHrP (107-111) loading onto HA_{Glu} scaffolds improves bone healing of a cavitary defect in the rat tibial metaphysis

3.2.1. μCT analysis

The bone tissue response to the implanted scaffolds tested was examined by μCT at the tissue/biomaterial interface and the peripheral area of the implant. We found that the PTHrP (107-111)-loaded scaffold completely healed the bone defect at 4 weeks after implantation. This contrasts with incomplete bone union observed by implanting the unloaded HA_{Glu} scaffold instead (Figs. 2A and 3A). Osteoinduction related to the presence of the PTHrP-derived pentapeptide on this scaffold was confirmed by quantitating the bone volume per total volume (BV/TV) at the cortical and trabecular compartments, as well as trabecular (Tb.Th) and cortical thickness (Ct.Th) (Figs. 2B and 3B), corresponding to at each skeletal site in the regenerating tibia, respectively.

3.2.2. Histological findings

At 4 weeks after implantation, no signs of inflammation were observed in the vicinity of HA_{Glu} materials. Complete repair of the cavitary bone defect was not observed in the unloaded HA_{Glu} control group at this time (Fig. 4A), though rats implanted with PTHrP (107-111)-loaded scaffolds showed good healing of the cavity (Fig. 4B). Consistent with the μCT results, the histological studies showed that, compared to the unloaded material, the implantation of PTHrP (107-111)-loaded HA_{Glu} scaffolds promoted the appearance of a lot more new trabeculae around the bone inte-

Please cite this article in press as: Lozano D et al. Parathyroid hormone-related protein (107-111) improves the bone regeneration potential of gelatin–glutaraldehyde biopolymer-coated hydroxyapatite. Acta Biomater (2014), http://dx.doi.org/10.1016/j.actbio.2014.03.025

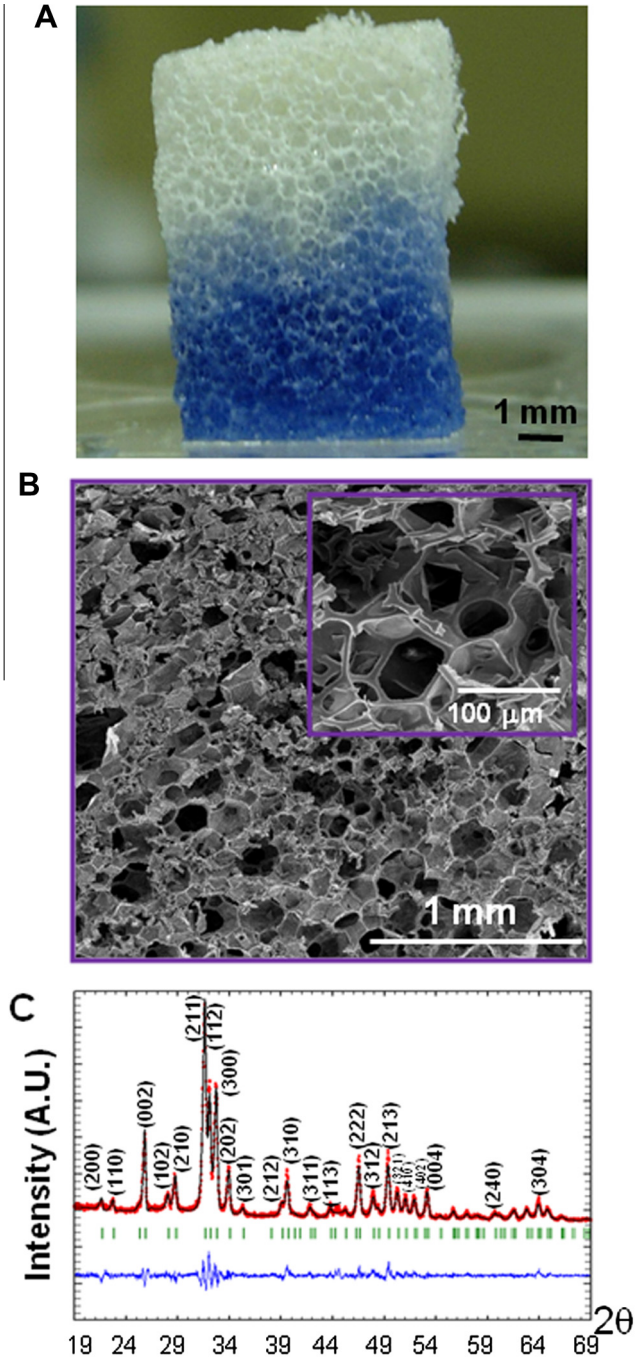

Fig. 1. (A) Representative digital micrograph of HA_{Glu} foams showing the diffusion of Trypan blue stain, changing the colour of the scaffold. (B) Representative SEM micrograph of HA_{Glu} foams. Inset: SEM micrograph at higher magnification (×200). (C) Experimental (symbols) and calculated (solid line) X-ray diffraction patterns of HA_{Glu} foams, obtained by Rietveld refinement. The lower trace is the difference between the observed and calculated patterns. The vertical lines mark the position of the calculated Bragg peaks for the apatite phase.

grated implants at 4 weeks (Fig. 4C–F). Furthermore, an increased number of osteoblasts together with less abundant osteoclasts were observed on trabecular surfaces in this healing bone area containing the pentapeptide-loaded scaffold (Fig. 5).

3.2.3. Changes in gene expression

The expression of several genes relevant in osteoblastic function was also examined in the rat tibial defect at 4 weeks post-implantation. The presence of PTHrP (107-111) in the implanted scaffolds was associated with augmented gene expression of both OC (a marker of osteoblast maturation) and VCAM 1 (an angiogenic factor) in the bony callus. The Wnt pathway has a key role in osteogenesis, and Wnt signalling has been shown to be functional early in the process of bone regeneration [36]. We found here that the gene expression of two important Wnt pathway inhibitors, Sost and DKK-1, was decreased in the injury callus with PTHrP (107-111)-loaded HA_{Glu} scaffolds (Fig. 6).

3.3. PTHrP (107-111) gives osteogenic features to HA_{Glu} scaffolds in osteoblastic cell cultures in vitro

In order to further confirm the observed osteogenic actions of PTHrP (107-111)-loaded HA_{Glu} scaffolds in bone regeneration in rats in vivo, we used osteoblastic cells cultures exposed to these biomaterials. Fig. 7A shows that MC3T3-E1 cell proliferation increased by loading PTHrP (107-111) onto HA_{Glu} scaffolds. Cell death, assessed by Trypan blue exclusion, was unchanged, at about 1%, in the presence of any of the tested scaffolds (data not shown). We next evaluated the capacity of this pentapeptide-loaded HA_{Glu} material to affect osteoblastic function. It was found that the presence of PTHrP (107-111) in the scaffold increased the expression of various genes related to osteoblast differentiation, namely OC and OPG, whereas it decreased that of RANKL – a key factor for inducing osteoclastogenesis – thereby increasing the OPG/RANKL mRNA ratio, at 4 days of culture (Fig. 7B). In addition, this type of scaffold containing this pentapeptide stimulated ALP activity at this time point in MC3T3-E1 cells (Fig. 8A), and promoted matrix mineralization in these cells and also in hOBs cells at day 12 of culture (Fig. 8B and inset). VEGF gene expression was also up-regulated in this scenario (Fig. 7B), which is consistent with the action of PTHrP (107-111) and the native PTHrP (107-139) fragment in various osteoblastic cell preparations [25,26,28,33,34]. The unloaded HA_{Glu} scaffolds failed to affect either cell growth or matrix mineralization in MC3T3-E1 cells within the time of the study (4–12 days), emphasizing the notion that PTHrP (107-111) gives bioactivity to these scaffolds (Figs. 7 and 8).

4. Discussion

Recently, we showed the osteoinductive actions of locally delivered PTHrP (107-111) from SBA15-based ceramics as implanted carriers into a rabbit bone defect [27,29]. This type of Si-enriched ceramic has a narrow mesopore size distribution (in the nanometre range) but a large surface area that governs the interaction with the host bone tissue. However, these materials were non-degradable and induced the formation of a thick fibrous cup around the implant [3,27,29]. This prompted us to evaluate whether loading PTHrP (107-111) into HA_{Glu} scaffolds would provide a more appropriate biomaterial as an implant for improving new bone formation. These scaffolds were therefore implanted into a cortical defect in the rat tibial metaphysis, in which bone regeneration is known to proceed through intramembranous ossification [12]. Using this approach, we demonstrate that PTHrP (107-111)-containing HA_{Glu} scaffolds display a clear advantage over peptide-unloaded scaffolds in promoting bone healing, as assessed by bone structure and histology, as well as molecular criteria. The cell autonomy of the osteogenic effects of this biomaterial was further confirmed using in vitro osteoblastic cell cultures.

An idoneous bone filler should provide structural support and a three-dimensional matrix to favour bone in- and on-growth, and gradually degrade to non-cytotoxic products [37,38]. Previous characterization of HA_{Glu} foamy scaffolds indicate that they fulfil these criteria [11,12]. In fact, the nanocrystalline structure of HA_{Glu} scaffolds, which is similar to that of native HA in bone, was found

Please cite this article in press as: Lozano D et al. Parathyroid hormone-related protein (107-111) improves the bone regeneration potential of gelatin–glutaraldehyde biopolymer-coated hydroxyapatite. Acta Biomater (2014), http://dx.doi.org/10.1016/j.actbio.2014.03.025

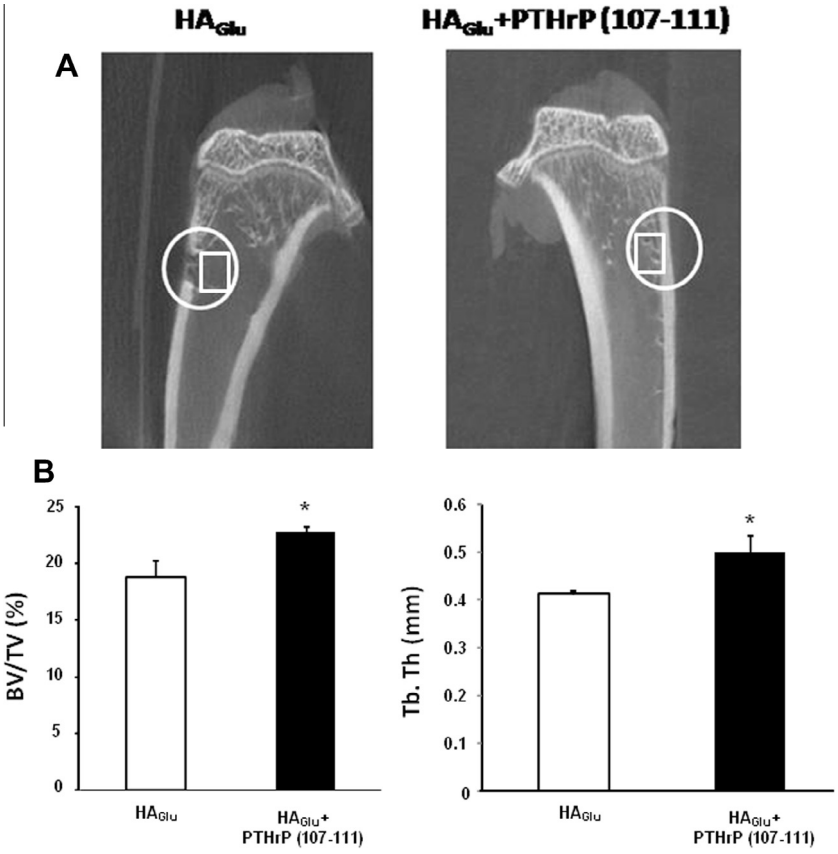

Fig. 2. (A) Representative frontal plane images by μCT of the area surrounding the HA_{Glu} implants, with or without loaded PTHrP (107-111), showing newly formed bone at 4 weeks after implantation into a cavitary defect in the rat tibia. (B) Trabecular bone volume/total volume (BV/TV) and trabecular thickness (Tb.Th) corresponding to the evaluated bone area around the implant. The circle denotes the bone defect, whereas the square shows the area close to the defect where the trabecular parameters were measured by μCT. Results are mean ± SE ($n = 5$). $^{*}p < 0.05$ vs. the corresponding unloaded HA_{Glu} scaffold.

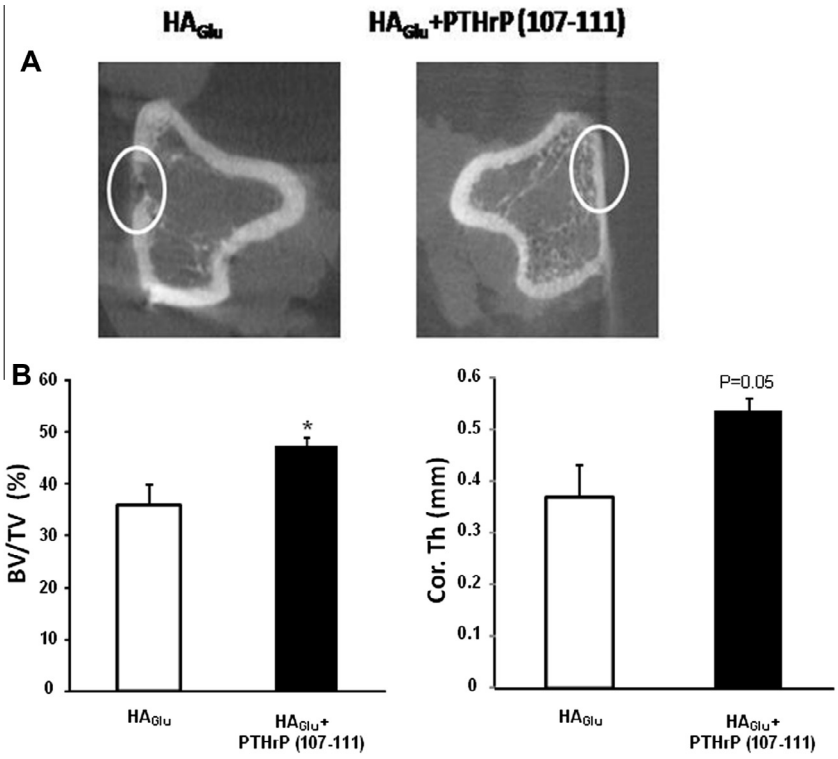

Fig. 3. (A) Representative transverse plane images by μCT of the area surrounding the HA_{Glu} implants, in the presence or absence of PTHrP (107-111), containing new bone at 4 weeks after implantation into a cavitary defect in the rat tibia. (B) Cortical bone volume/total volume (BV/TV) and cortical thickness (Ct.Th) corresponding to the evaluated bone area around the implant as remarked by the circle. Results are mean ± SE ($n = 5$). $^{*}p < 0.05$ vs. the corresponding unloaded HA_{Glu} scaffold.

Please cite this article in press as: Lozano D et al. Parathyroid hormone-related protein (107-111) improves the bone regeneration potential of gelatin–glutaraldehyde biopolymer-coated hydroxyapatite. Acta Biomater (2014), http://dx.doi.org/10.1016/j.actbio.2014.03.025

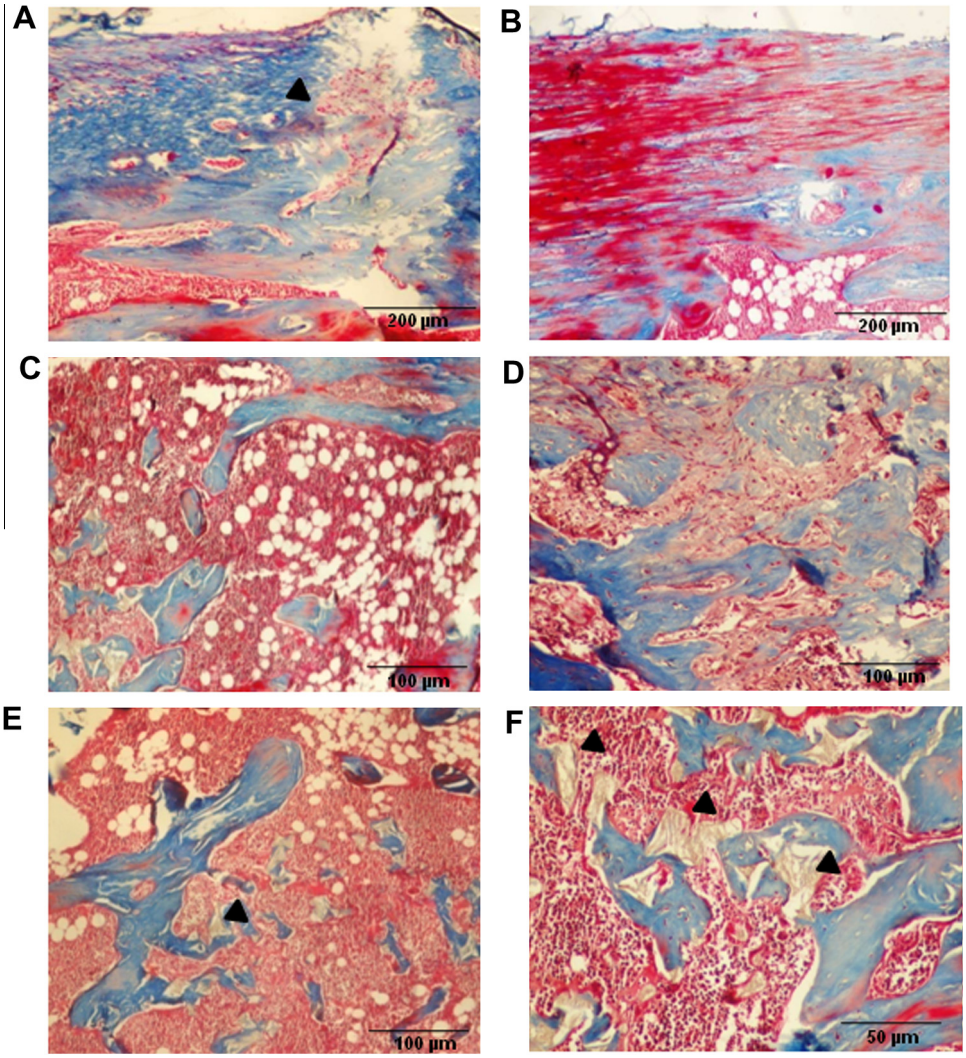

Fig. 4. Representative images by light microscopy (from haematoxylin & eosin and Masson's stained tissue sections) of the area surrounding the unloaded (A and C) and loaded (B, D, E and F) with PTHrP (107-111) HA_{Glu} scaffolds 4 weeks after implantation into a cavitary defect in the rat tibia. Arrows denote the presence of HA_{Glu} scaffold.

to promote bone formation, avoiding the generation of fibrous tissue around the implant [12]. The biological performance of HA_{Glu} scaffolds allows their definition as third-generation materials for orthopaedic use [39]. It was recently found that these scaffolds display excellent osteointegration properties when implanted into a cavitary bone defect in the rabbit epiphysis; thus, complete bone healing was observed at 4 months after implantation [12]. In the present study, we examined the performance of both types of implants tested – with and without PTHrP (107-111) – in a rat cortical bone defect at 4 weeks, which is an insufficient time period for complete bone healing [40]. This approach allowed us to more easily disclose the osteoinductive advantage represented by the PTHrP (107-111)-loaded foams.

Dramatic differences were observed in the pattern of bone repair of this non-critical bone defect in the rat tibia between both types of implanted HA_{Glu} scaffold evaluated. The occurrence of bone regeneration leading to a completely sealed cortical defect was strictly associated with the presence of PTHrP (107-111) in the scaffold after 4 weeks. Consistent with previous data using other types of non-degradable ceramics as carriers of this pentapeptide [26], we observed here that, in vitro, PTHrP (107-111) was released very rapidly (within 2 days) from HA_{Glu} scaffolds into the surrounding medium. Using the former materials, even small amounts of this peptide (in the nanomolar range or lower concentrations) remaining in the non-degradable ceramic seemed to elicit osteogenic actions [26,27,29]. The HA_{Glu} scaffolds have been shown to be stable for about 2 weeks, but progressive degradation occurs thereafter [11]. Thus, and consistent with previous observations in a rabbit model [12], we found here, using μCT and histological analysis, scarce HA_{Glu} material (although still detectable) in the bone defect area in our rat model at 4 weeks after implantation. Most proposed release strategies (i.e. using BMP2) provide a burst immediately after the local (surgical) application [41]. However, it is presently debatable whether maintaining the peptide bioactivity and its release burst are equally important factors in this respect. Assuming similar PTHrP (107-111) kinetics in our present in vivo setting, it seems that, besides the initial burst, even the remaining material containing a small amount of this peptide in the 2 days to 4 weeks time frame might contribute to improving bone healing in this model.

Our present data show that PTHrP (107-111)-loaded HA_{Glu} scaffolds promote trabecular formation, with abundant osteoblastic cells adhering to the trabecular surface in the vicinity of the degrading biomaterial. This was related to an increased gene expression of OC, a late osteoblast differentiation marker, and accompanied by gene overexpression of VCAM 1, a vascular endothelial marker [42], in the regenerated callus. In this regard, previous studies have shown that local or systemic administration of

Please cite this article in press as: Lozano D et al. Parathyroid hormone-related protein (107-111) improves the bone regeneration potential of gelatin–glutaraldehyde biopolymer-coated hydroxyapatite. Acta Biomater (2014), http://dx.doi.org/10.1016/j.actbio.2014.03.025

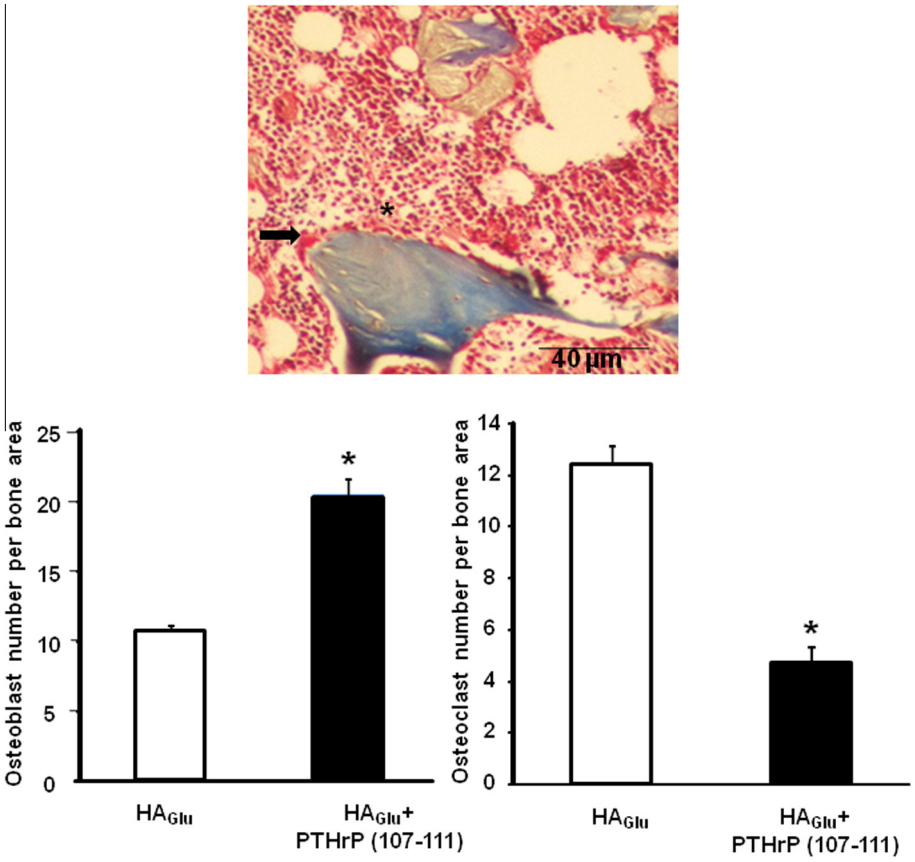

Fig. 5. Relative abundance of osteoblasts and osteoclasts observed on trabecular surfaces in the bone healing area around each type of implanted HA_{Glu} scaffold into a cavitary defect in the rat tibia (as described in the legend to Fig. 2), 4 weeks after implantation. The arrow and the star denote the presence of multinucleated osteoclast and cuboidal osteoblasts, respectively. Results are mean ± SE ($n = 5$). $^{*}p < 0.05$ vs. the corresponding unloaded HA_{Glu} scaffold.

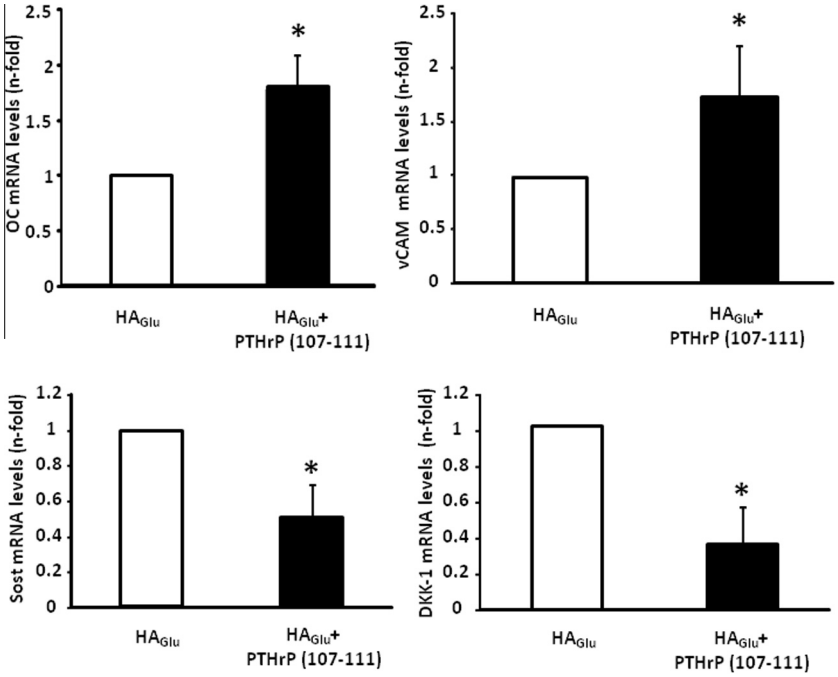

Fig. 6. Gene expression (by real-time PCR) of bone-related factors and the angiogenic factor VCAM 1 in the callus generated at 4 weeks after implantation of PTHrP (107-111)-loaded or unloaded HA_{Glu} scaffolds into a cavitary defect in the rat tibia. Results are mean ± SE ($n = 5$). $^{*}p < 0.05$ vs. the corresponding unloaded HA_{Glu} scaffold.

Please cite this article in press as: Lozano D et al. Parathyroid hormone-related protein (107-111) improves the bone regeneration potential of gelatin–glutaraldehyde biopolymer-coated hydroxyapatite. Acta Biomater (2014), http://dx.doi.org/10.1016/j.actbio.2014.03.025

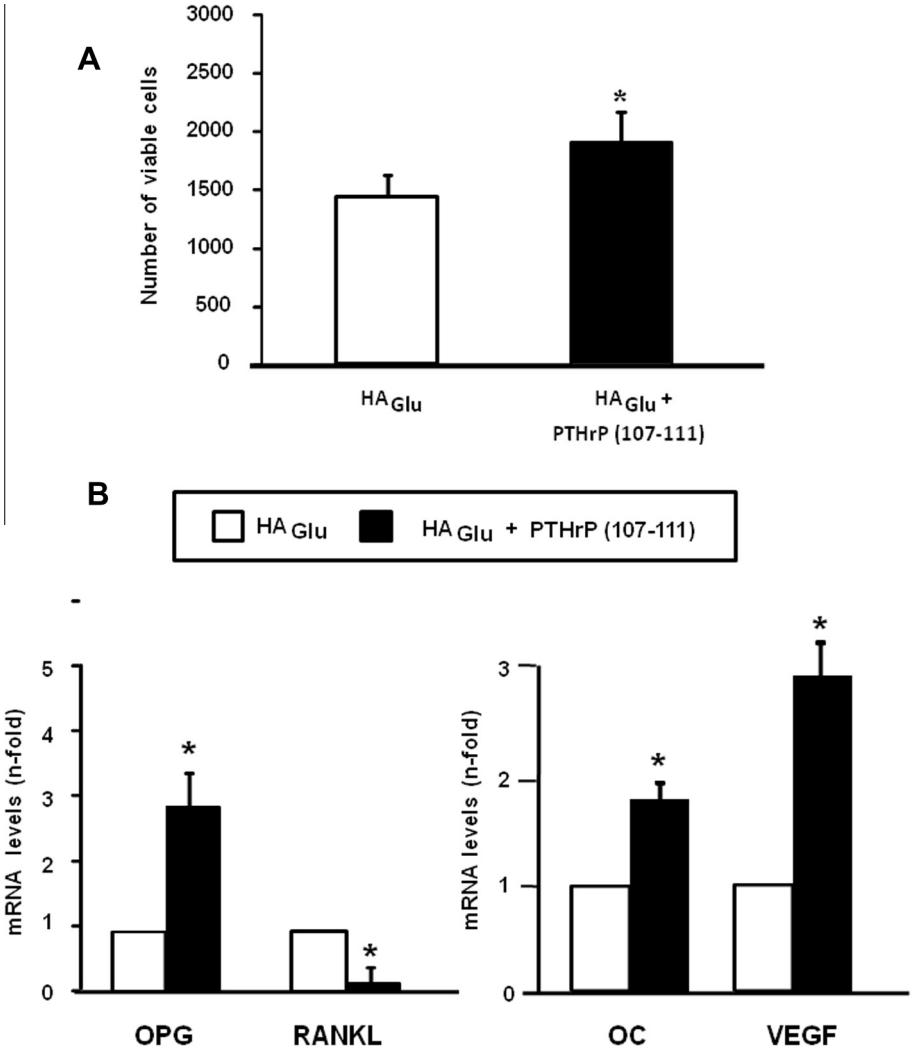

Fig. 7. Changes in osteoblast viability and osteoblast function-related genes induced by the presence of PTHrP (107-111) on HA_{Glu} scaffolds in MC3T3-E1 cells. Cell viability was measured by Trypan blue exclusion (A), and OC, VEGF, OPG and RANKL mRNA levels were determined by real-time PCR (B) at day 4 of culture. Results are mean ± SE of three independent experiments performed in triplicate. $^{*}p < 0.05$ vs. the corresponding unloaded HA_{Glu} scaffold.

PTHrP (107-111) or the native PTHrP (107-139) fragment, respectively, increased angiogenesis in other in vivo models of bone regeneration in mice and rabbits [19,20,27,29]. The present in vitro data further support the idea that PTHrP (107-111) loading confers osteogenic and angiogenic potential to HA_{Glu} foams.

PTHrP (107-111)-loaded HA_{Glu} scaffolds induced the opposite effect (i.e. a decrease) on two well-known inhibitors of the canonical Wnt pathway, DKK1 and Sost, in the healing bone defect. Of note, the putative PTHrP (107-139) fragment has been reported to decrease the expression of both genes in bone after its systemic administration for 4 weeks to ovariectomized mice, and also in rat osteoblastic UMR-106 cells [21]. Moreover, Sost downregulation has been shown to be an important event in the early phase of fracture healing in humans [43]. Furthermore, a previous study demonstrates that systemic or local injection of a DKK1 adenovirus hampered cortical defect healing in the mouse tibial diaphysis [36]. It has also been shown that an anti-DKK1 antibody injection was efficient to stimulate bone healing after trauma caused by a stainless steel screw inserted into the rat tibial metaphysis [44]. Hence, our present findings add credence to the notion that PTHrP (107-111) loaded onto HA_{Glu} scaffolds may promote bone healing through targeting the Wnt pathway.

Our results also indicate that PTHrP (107-111) loading onto HA_{Glu} scaffolds decreased the abundance of osteoclasts resorbing new bone around the implant. This was not surprising, considering the ability of this peptide to reduce the number of trabecular osteoclasts when administered subcutaneously, as recently reported [45], and the observed increase in OPG/RANKL mRNA ratio induced by PTHrP (107-111)-loaded HA_{Glu} scaffolds in osteoblast cultures in this work. In fact, PTHrP (107-139) has consistently been shown to display anti-resorptive features in rodents [17,20–22], apparently by interacting with osteoclasts directly or indirectly through targeting osteoblasts [19,23,26,28]. Also in this regard, the local presence of PTHrP (107-111) was shown to inhibit the transient inflammatory response as well as the appearance of osteoclasts in a cavitary bone defect in the rabbit femur [27]. Together these data strongly suggest that PTHrP (107-111) may inhibit osteoclastogenesis during bone regeneration.

5. Conclusions

The present findings demonstrate the suitability of our experimental combined strategy, adding credence to the notion that loading these degradable HA_{Glu} scaffolds with PTHrP (107-111)

Please cite this article in press as: Lozano D et al. Parathyroid hormone-related protein (107-111) improves the bone regeneration potential of gelatin–glutaraldehyde biopolymer-coated hydroxyapatite. Acta Biomater (2014), http://dx.doi.org/10.1016/j.actbio.2014.03.025

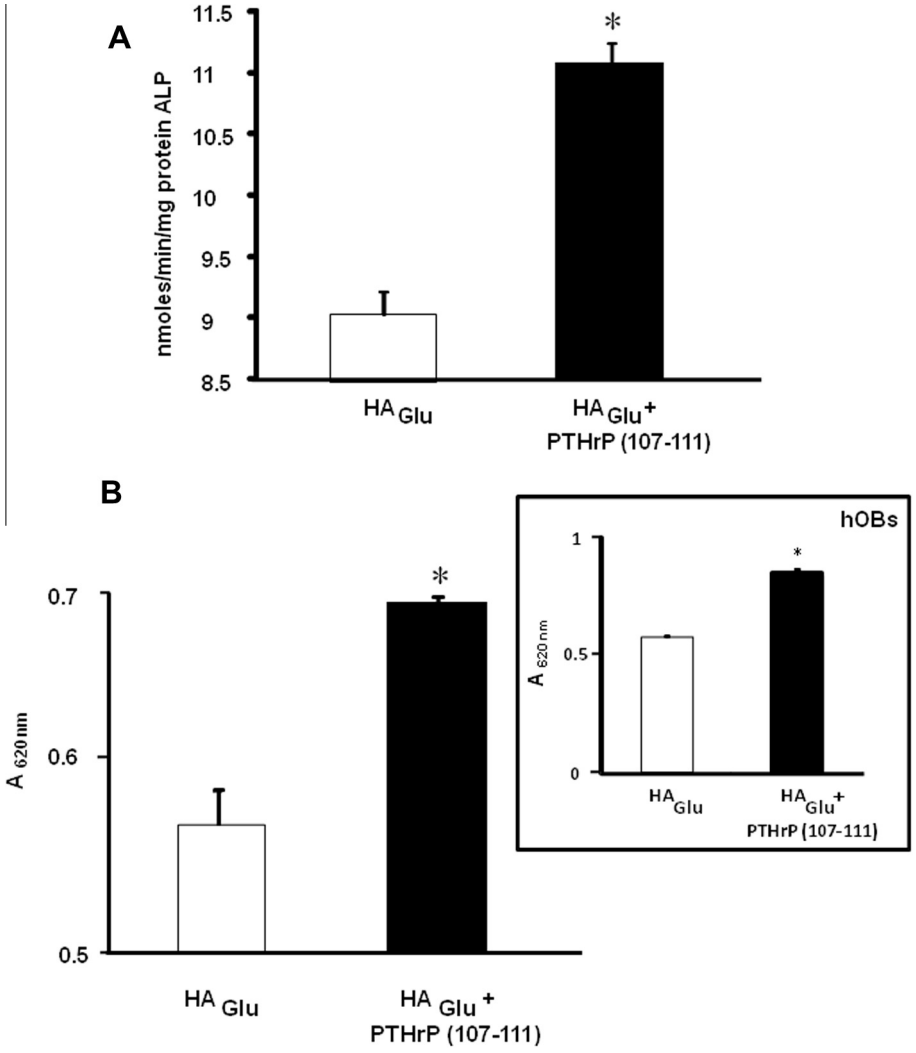

Fig. 8. (A) Changes in osteoblast differentiation induced by the presence of PTHrP (107-111) on HA_{Glu} scaffolds in osteoblastic cell cultures. ALP activity (A) and matrix mineralization (B) were measured in the presence of HA_{Glu} loaded or not with PTHrP (107-111) in MC3T3-E1 cells at day 4 and 12 of culture, respectively, and hOB cells after 12 days, as described in the text. Results are mean ± SE of three independent experiments performed in triplicate. $^{*}p < 0.05$ vs. the corresponding unloaded HA_{Glu} scaffold.

produces an optimal cavity filling biomaterial that is promising in low load bearing clinical applications.

Acknowledgements

The Spanish and European Network of Excellence for the Prevention and Treatment of Osteoporotic Fractures "Ageing" is financially supported by the Ministerio de Economía y Competitividad through the project CSO2010-11384-E. This research was supported by Grants from the Ministerio de Ciencia e Innovación (MAT2012-35556), Ministerio de Economía y Competitividad (RETICEF RD12/0043/0008) and Comunidad Autónoma de Madrid (S2009 MAT-1472). D.L., S.P.-N. and J.A.A. are recipients of postdoctoral research contracts from Comunidad Autónoma de Madrid (S-2009/Mat-1472), RETICEF (RD06/0013/1002 and RD12/0043/0008) and Ministerio de Ciencia e Innovación-Juan de la Cierva program (JCI-2011-09548), respectively. A.L.-H. was supported by Fundación Conchita Rábago and Ministerio de Educación-FPU program (AP2009-1871). We are indebted to Dr. C. Castilla (Animal Facility, IIS-Fundación Jiménez Díaz) for expert advice on the surgical procedures.

Appendix A. Supplementary data

Supplementary data associated with this article can be found, in the online version, at http://dx.doi.org/10.1016/j.actbio.2014.03.025.

Appendix B. Figures with essential colour discrimination

Certain figures in this article, particularly Figs. 1, 4 and 5 are difficult to interpret in black and white. The full colour images can be found in the on-line version, at http://dx.doi.org/10.1016/j.actbio.2014.03.025.

References

[1] The Bone and Joint Decade, 2005. www.boneandjointdecade.org.
[2] Arvidson K, Abdallah BM, Applegate LA, Nicola Baldini N, Cenni E, Gomez-Barrena, et al. Bone regeneration and stem cells. J Cell Mol Med 2011;15:718–46.
[3] Salinas AJ, Esbrit P, Vallet-Regí M. A tissue engineering approach based on the use of bioceramics for bone repair. Biomater Sci 2013;1:40–51.
[4] Portal-Núñez S, Lozano D, Esbrit P. Role of angiogenesis in bone formation. Histol Histopathol 2012;27:559–66.

[5] Vallet-Regí M, Ruiz-Hernández E. Bioceramics: from bone regeneration to cancer nanomedicine. Adv Mater 2011;23:5177–218.
[6] Vallet-Regi M, Salinas AJ. Ceramics and bone repair. In: Planell JA, Best SM, Lacroix D, Merolli A, editors. Bone repair biomaterials. Boca Raton, FL: CRC Press; 2009. p. 194–230.
[7] Hench L, Polak JM. Third-Generation Biomedical Materials. Science 2002;295:1014–7.
[8] Albrektsson T, Johansson C. Osteoinduction, osteoconduction and osseointegration. Eur Spine J 2001;10:96–101.
[9] Sánchez-Salcedo S, Vila M, Izquierdo-Barba I, Cicuéndez M, Vallet-Regí M. Biopolymer-coated hydroxyapatite foams: a new antidote for heavy metal intoxication. J Mater Chem 2010;20:6956–61.
[10] Vila M, Sánchez-Salcedo S, Cicuéndez M, Izquierdo-Barba I, Vallet-Regí M. Novel biopolymers-coated hydroxyapatite foams for removing heavy metals from polluted water. J Hazard Mater 2011;192:71–7.
[11] Cicuéndez M, Izquierdo-Barba I, Sánchez-Salcedo S, Vila M, Vallet-Regí M. Biological performance of hydroxyapatite–biopolymer foams: in vitro cell response. Acta Biomater 2012;8:802–10.
[12] Gil-Albarova J, Vila M, Badiola-Vargas J, Sánchez-Salcedo S, Herrera A, Vallet-Regi M. In vivo osteointegration of three-dimensional crosslinked gelatin-coated hydroxyapatite foams. Acta Biomater 2012;8:3777–83.
[13] Schieker M, Seitz H, Drosse I, Seitz S, Mutschler W. Biomaterials as scaffold for bone tissue engineering. Eur J Trauma 2006;32:114–24.
[14] Driscoll P. Orthopedic biomaterials market growth strongest in US. 2009. http://mediligence.com/blog/2009/01/30/orthopedic-biomaterials-market-growth-strongest-in-us/.
[15] Esbrit P, Alcaraz MJ. Current perspectives on parathyroid hormone (PTH) and PTH-related protein (PTHrP) as bone anabolic therapies. Biochem Pharmacol 2013;85:1417–23.
[16] Datta NS, Abou-Samra AB. PTH and PTHrP signaling in osteoblasts. Cell Signal 2009;21:245–54.
[17] Cornish J, Callon KE, Nicholson GC, Reid IR. Parathyroid hormone-related protein-(107–139) inhibits bone resorption in vivo. Endocrinology 1997;138:1299–304.
[18] Cornish J, Callon KE, Lin C, Xiao C, Moseley JM, Reid IR. Stimulation of osteoblast proliferation by C-terminal fragments of parathyroid hormone-related protein. J Bone Miner Res 1999;14:915–22.
[19] Lozano D, Fernández-de-Castro L, Portal-Núñez S, López-Herradón A, Dapía S, Gómez-Barrena E, et al. The C-terminal fragment of parathyroid hormone-related peptide promotes bone formation in diabetic mice with low turnover osteopenia. Br J Pharmacol 2011;162:1424–38.
[20] de Castro LF, Lozano D, Dapía S, Portal-Núñez S, Caeiro JR, Gómez-Barrena E, et al. Role of the N- and C-terminal fragments of parathyroid hormone-related protein as putative therapies to improve bone regeneration under high glucocorticoid treatment. Tissue Eng Part A 2010;16:1157–68.
[21] Decastro LF, Lozano D, Portal-Núñez S, Maycas M, DelaFuente M, Caeiro JR, et al. Comparison of the skeletal effects induced by daily administration of PTHrP (1–36) and PTHrP (107–139) to ovariectomized mice. J Cell Physiol 2012;227:1752–60.
[22] Rihani-Basharat S, Lewinson D. PTHrP (107-111) inhibits in vivo resorption that was stimulated by PTHrP (1-34) when applied intermittently to neonatal mice. Calcif Tissue Int 1997;61:426–8.
[23] Fenton AJ, Kemp BE, Kent GN, Moseley JM, Zheng MH, Rowe DJ, et al. A carboxyl-terminal peptide from the parathyroid hormone-related protein inhibits bone resorption by osteoclasts. Endocrinology 1991;129:1762–8.
[24] Valín A, Guillén C, Esbrit P. C-terminal parathyroid hormone-related protein (PTHrP) (107-139) stimulates intracellular Ca^{2+} through a receptor different from the type 1 PTH/PTHrP receptor in osteoblastic osteosarcoma UMR 106 cells. Endocrinology 2001;142:2752–9.
[25] García-Martín A, Acitores A, Maycas M, Villanueva-Peñacarrillo ML, Esbrit P. Src kinases mediate VEGFR2 transactivation by the osteostatin domain of PTHrP to modulate osteoblastic function. J Cell Biochem 2013;114:1404–13.
[26] Lozano D, Manzano M, Doadrio JC, Salinas AJ, Vallet-Regí M, Gómez-Barrena E, et al. Osteostatin-loaded bioceramics stimulate osteoblastic growth and differentiation. Acta Biomater 2010;6:797–803.
[27] Trejo CG, Lozano D, Manzano M, Doadrio JC, Salinas AJ, Dapía S, et al. The osteoinductive properties of mesoporous silicate coated with osteostatin in a rabbit femur cavity defect model. Biomaterials 2010;31:8564–73.
[28] De Gortázar AR, Alonso V, Alvarez-Arroyo MV, Esbrit P. Transient exposure to PTHrP (107-139) exerts anabolic effects through vascular endothelial growth factor receptor 2 in human osteoblastic cells in vitro. Calcif Tissue Int 2006;79:360–9.
[29] Lozano D, Trejo CG, Gómez-Barrena E, Manzano M, Doadrio JC, Salinas AJ, et al. Osteostatin-loaded onto mesoporous ceramics improves the early phase of bone regeneration in a rabbit osteopenia model. Acta Biomater 2012;8:2317–23.
[30] Brinker CJ, Lu YF, Sellinger A, Fan HY. Evaporation-induced self-assembly: nanostructures made easy. Adv Mater 1999;11:579–85.
[31] Thompson Z, Miclau T, Hu D, Helms JA. A model for intramembranous ossification during fracture healing. J Orthop Res 2002;20:1091–8.
[32] Chou J, Hao J, Kuroda S, Bishop D, Ben-Nissan B, Milthorpe B, et al. Bone regeneration of rat tibial defect by zinc-tricalcium phosphate (Zn-TCP) synthesized from porous Foraminifera carbonate macrospheres. Mar Drugs 2013;11:5148–58.
[33] López-Herradón A, Portal-Núñez S, García-Martín A, Lozano D, Pérez-Martínez FC, Ceña V, et al. Inhibition of the canonical Wnt pathway by high glucose can be reversed by parathyroid hormone-related protein in osteoblastic cells. J Cell Biochem 2013;114:1908–16.
[34] Lozano D, Feito MJ, Portal-Núñez S, Lozano RM, Matesanz MC, Serrano MC, et al. Osteostatin improves the osteogenic activity of fibroblast growth factor-2 immobilized on Si-doped hydroxyapatite in osteoblastic cells. Acta Biomater 2012;8:2770–7.
[35] Rodríguez-Carvajal J. Recent advances in magnetic structure determination by neutron powder diffraction. Physica B 1993;192:55–69.
[36] Kim J-B, Leucht P, Lam K, Luppen C, Berge DT, Nusse R, et al. Bone regeneration is regulated by Wnt signaling. J Bone Miner Res 2007;22:1913–23.
[37] Nejati E, Firouzdor V, Eslaminejad MB, Bagheri F. Needle-like nano hydroxyapatite/poly(L-lactide acid) composite scaffold for bone tissue engineering application. Mater Sci Eng C 2009;293:942–9.
[38] Shors EC. Coraline bone graft substitutes. Orthop Clin North Am 1999;30:599–613.
[39] Vallet-Regí M. Evolution of bioceramics within the field of biomaterials. C R Chim 2010;13:174–85.
[40] Pearce AI, Richards RG, Milz S, Schneider E, Pearce SG. Animal models for implant biomaterial research in bone: a review. Eur Cell Mater 2007;13:1–10.
[41] Uludag H, D'Augusta D, Palmer R, Timony G, Wozney J. Characterization of rhBMP-2 pharmacokinetics implanted with biomaterial carriers in the rat ectopic model. Biomed Mater Res 1999;46:193–202.
[42] Liekens S, De Clercq E, Neyts J. Angiogenesis: regulators and clinical applications. Biochem Pharmacol 2001;61:253–70.
[43] Caetano-Lopes J, Lopes A, Rodrigues A, Fernandes D, Perpétuo IP, Monjardino T, et al. Upregulation of inflammatory genes and downregulation of sclerostin gene expression are key elements in the early phase of fragility fracture healing. PLoS One 2011;6:e16947.
[44] Agholme F, Isaksson H, Kuhstoss S, Aspenberg P. The effects of Dickkopf-1 antibody on metaphyseal bone and implant fixation under different loading conditions. Bone 2011;48:988–99.
[45] Rodríguez-de la Rosa L, López-Herradón A, Portal-Núñez S, Murillo-Cuesta S, Lozano D, Cediel R, et al. Treatment with N- and C-terminal peptides of parathyroid hormone-related protein partly compensate the skeletal abnormalities in igf-I deficient mice. PLoS One 2014;9:e87536.

Please cite this article in press as: Lozano D et al. Parathyroid hormone-related protein (107-111) improves the bone regeneration potential of gelatin–glutaraldehyde biopolymer-coated hydroxyapatite. Acta Biomater (2014), http://dx.doi.org/10.1016/j.actbio.2014.03.025